Dissociative Chemisorption and Energy Transfer for Methane on Ir(111)

Heather L. Abbott and Ian Harrison*

Department of Chemistry, University of Virginia, Charlottesville, Virginia 22904-4319

Received: January 31, 2005

A 3-parameter local hot spot model of gas−surface reactivity is employed to analyze and predict dissociative sticking coefficients for CH_4 incident on Ir(111) under varied nonequilibrium and equilibrium conditions. One Ir surface oscillator and the molecular vibrations, rotations, and translational energy directed along the surface normal are treated as active degrees of freedom in the 14 dimensional microcanonical kinetics. The threshold energy for CH_4 dissociative chemisorption on Ir(111) derived from modeling molecular beam experiments is $E_0 = 39$ kJ/mol. Over more than 4 orders of magnitude of variation in sticking, the average relative discrepancy between the beam and theoretically derived sticking coefficients is 88%. The experimentally observed enhancement in dissociative sticking as beam translational energies decrease below ∼10 kJ/mol is consistent with a parallel dynamical trapping/energy transfer channel that likely fails to completely thermalize the molecules to the surface temperature. This trapping-mediated sticking, indicative of specific energy transfer pathways from the surface under nonequilibrium conditions, should be a minor contributor to the overall dissociative sticking at thermal equilibrium. Surprisingly, the CH_4 dissociative sticking coefficient predicted for Ir(111) surfaces at thermal equilibrium, based on the molecular beam experiments, is roughly 4 orders of magnitude higher than recent measurements on supported nanoscale Ir catalysts at 1 bar pressure, which suggests that substantial improvements in catalyst turnover rates may be possible.

I. Introduction

Achieving a comprehensive understanding of the activated dissociative chemisorption of methane on catalytic metal surfaces has been a long-standing scientific and technological aspiration because of the reaction's central role in the industrial reforming of natural gas, the process principally responsible for the commercial supply of H_2 and synthesis gas (a mixture of H_2 and CO).[1] Under high-pressure industrial conditions, the sole kinetically relevant step in the catalytic dry or steam reforming of methane is the initial C−H bond cleavage, and the catalyst turnover frequency is found to depend only on the methane partial pressure.[2−7] Although supported nickel nanocrystallites are the primary catalyst used in industrial reforming, iridium displays higher activity.[5] Molecular beam studies of methane dissociative chemisorption on single-crystal metal surfaces[1] have typically been interpreted in terms of a "direct" mechanism in which the reactive energy barrier is surmounted promptly during the initial gas−surface collision, but for some Ir and Pt surfaces a parallel "thermal trapping" mechanism has been invoked to account for the initial decrease in the methane dissociative sticking coefficient, S, as the normal translational energy, E_n, is increased from 0 to ∼10 kJ/mol.[8] For CH_4 dissociative chemisorption on Ir(111), a key experimental observation is an unusual V-shaped curve for log S versus E_n with a minimum near 10 kJ/mol.[9]

The literature provides no consensus value for the activation energy for methane dissociative chemisorption on Ir(111), but rather, it suggests a range from 15 to 81 kJ/mol. Seets et al.[9] and Jachimowski et al.[10] report "effective activation energies" of "E_a" = 27 ± 4 kJ/mol and "E_a" = 53 kJ/mol, respectively, obtained from Arrhenius fits to the nonequilibrium sticking observed in "bulb" experiments where T_s was varied and T_g = 300 K was held fixed. Jachimowski et al. also report a thermal activation energy of $E_a = 72$ kJ/mol, while recent experiments performed by Wei and Iglesia[6,7] on supported Ir nanocrystallite catalysts indicate a thermal activation energy of $E_a = 81$ kJ/mol. Density functional theory (DFT) calculations by Henkelman and Jónsson[11] and Au et al.[12] gave reaction threshold energy E_0 (=E_a at 0 K) values of 15 ± 10 and 76 kJ/mol, respectively. The wide range of activation energies, suggested by both experiment and theory, makes it difficult to make credible kinetic predictions, because any error in an activation energy is exponentially amplified. A further complication is that reported preexponential factors for thermal sticking vary by many orders of magnitude.

In this manuscript, we apply a recently developed three-parameter physisorbed complex - microcanonical unimolecular rate theory (PC-MURT)[13] to analyze and predict dissociative sticking coefficients for the dissociative chemisorption of CH_4 on Ir(111). The PC-MURT provides a statistical description of the surface reaction dynamics, recovers canonical transition-state theory and Arrhenius sticking coefficients for thermal systems, and provides a baseline against which nonstatistical behavior[14,15] can be identified when it occurs. The ability of the PC-MURT to simulate both thermal equilibrium and nonequilibrium experiments in a unified manner provides opportunities to define transition-state characteristics on the basis of input from a wide variety of experiments and to directly compare the results derived from dissimilar experiments. In earlier work, the PC-MURT was successfully employed to quantitatively predict experimental dissociative sticking coefficients (accurate to ca. 50%) for methane on Pt(111)[13] and Ni(100),[16−18] and for silane on Si(100),[19] over a broad range of experiments spanning some ten orders of magnitude variation in sticking and pressure. Here, the PC-MURT applied to the

* Phone: (434) 924-3639. Fax: (434) 924-3966. Electronic mail: harrison@virginia.edu.

10.1021/jp0505375 CCC: $30.25
Published on Web 04/21/2005

CH_4/Ir(111) system is employed to (i) derive a 39 kJ/mol threshold energy for dissociative chemisorption that may serve as a benchmark for electronic structure theory calculations, (ii) compare disparate ultrahigh-vacuum surface science and high-pressure catalysis experiments, (iii) predict from what molecular and surface degrees of freedom the energy required to overcome the activation barrier for dissociation is drawn, and (iv) explore the nature of the thermal trapping sticking mechanism observed at low E_n.

The PC-MURT presumes the gas−surface chemistry is a local phenomenon in which an incident molecule interacts with only a few surface oscillators to form a transient "local hot spot" or "physisorbed complex" (PC) whose ultrafast lifetime at the reactive energies of interest ($\tau_D \approx 2$ ps) serves to limit energy exchange with the surrounding bulk.[13,18] In an ensemble-averaged sense, energy within the PCs is assumed to be microcanonically and adiabatically randomized by the initial collisions,[20] rapid intramolecular vibrational energy redistribution (IVR),[13] or both.[13,18] PCs formed at a particular energy E^* are subject to competitive dissociation and desorption with Rice−Ramsperger−Kassel−Marcus (RRKM) rate constants, $k_i(E^*)$. Thus, the PC-MURT amounts to a "microcanonical" trapping mechanism in which the local energy of a PC becomes microcanonically randomized (but not thermalized to the surface temperature) and the competition between dissociation and desorption defines the dissociative sticking coefficient. A more sophisticated master equation (ME)-MURT has been developed to allow for the possibility of thermalization of the PCs within the physisorption potential well through weak collisional energy coupling with the surrounding bulk.[13] To date, PC/bulk energy transfer has been estimated as being sufficiently slow to be ignorable. However, for the far from thermal equilibrium CH_4/Ir(111) molecular beam experiments of Seets et al. with $T_s = 1000$ K and $E_n \leq 10$ kJ/mol, the dissociative sticking enhancement as E_n is reduced provides suggestive indirect evidence for energy transfer from the surface bulk to the PCs (i.e., energy transfer toward thermalization of the PCs to T_s).

A quite different *dynamical* thermal trapping mechanism has frequently been applied to dissociative chemisorption systems involving a physisorbed precursor state where the activation energy for dissociative chemisorption, E_{aR}, lies below the activation energy for desorption from the physisorption potential well, E_{aD}.[21] In this thermal trapping mechanism, molecules are first trapped into the physisorption well, somehow thermalized to the surface temperature in an unspecified manner, and then subject to competitive thermal dissociation reaction and desorption with Arrhenius rate constants, $k_i(T_s) = A_i \exp(-E_{ai}/k_b T_s)$. The dissociative sticking coefficient for thermal trapping is given by

$$S(E, \vartheta; T_s) = \zeta(E, \vartheta; T_s) \frac{k_R(T_s)}{k_R(T_s) + k_D(T_s)}$$

$$S = \zeta\left(1 + \frac{k_D}{k_R}\right)^{-1} = \zeta\left[1 + \frac{A_D}{A_R}\exp\left(-\frac{E_{aD} - E_{aR}}{k_b T_s}\right)\right]^{-1} \quad (1)$$

in which the trapping coefficient, $\zeta(E, \vartheta; T_s)$, may depend on the energy and quantum states of the incident molecule, its angle of incidence, and the surface temperature, and the second bracketed term is an explicit function of the surface temperature alone. At a minimum, the thermal trapping mechanism employs three parameters, $\{\zeta, A_D/A_R, E_{aD} - E_{aR}\}$, with all the dynamical information residing in ζ which may have a complicated functionality.[22] Unfortunately, ζ has never been experimentally characterized for methane at reactive surface temperatures. As the incident molecular translational energy is increased, it should become increasingly difficult to trap and thermalize molecules within the physisorption well, and so, ζ and S should decrease with increasing translational energy. Another signature of thermal-trapping-mediated sticking is a decrease in the sticking as the surface temperature is increased for typical chemisorption systems with $E_{aR} < E_{aD}$. Unusually, Seets et al.[9] observed that at low translational energies of methane incident on Ir(111) the sticking increases as the surface temperature increases in accord with eq 1 and activated chemisorption with $E_{aR} > E_{aD}$. Classical molecular dynamics simulations[22] for methane trapping on Ir(111) predict that the trapping coefficient is greater than 0.1 for normal translational energies $E_n \leq 10$ kJ/mol and essentially independent of surface temperature over the range 300 K $\leq T_s \leq$ 1000 K. Jachimowski et al.[10] argue that the trapping probability on Ir(111) can be taken as $\zeta \approx 1$ at these low incident translational energies. However, it is far from clear how trapped methane at the Ir(111) surface can thermalize and maintain a canonical thermal distribution during the eq 1 kinetics at energies appropriate to reaction (i.e., $E \geq E_{aR}$), because the much lower desorption energy (n.b., $E_{aR} - E_{aD} \approx E_0 = 39$ kJ/mol) should lead to rapid desorptive loss of high-energy molecules.

After the experimental report that N_2 dissociative chemisorption at 500 K is 9 orders of magnitude more probable at the steps of Ru(0001) as compared to the terraces,[23] it has been tempting to conclude that surface science studies are typically dominated by reactivity at steps, and in turn, such steps must dominate the reactivity of commercial catalysts. However, such a generalization would be premature to extend to methane dissociative chemisorption on the basis of current experimental evidence.[24] Nørskov[25] has recently proposed some universality rules for choosing prospective catalysts, in part, on the basis of the idea that step sites will dominate dissociative chemistry at surfaces, unless the steps are poisoned in some way. The same rules predict that the steps will be rapidly poisoned because of the stronger, and possibly irreversible, binding of the dissociation products at the steps. Recent generalized gradient approximation density functional theory (GGA-DFT) calculations predict that the threshold energy for CH_4 dissociative chemisorption should fall 30 kJ/mol at the step sites of Pd(111) and Rh(111).[26] A molecular beam study of CH_4 dissociative chemisorption on Pt(553) claims a similar ~30 kJ/mol reduction of the dissociation threshold energy at the steps of this surface composed of (111) terraces and (100) steps based on a semiempirical theoretical analysis.[27] In light of these reports, it is reasonable to question whether the trapping-mediated sticking observed on CH_4/Ir(111) at low E_n derives not from energy transfer during the lifetime of the trapped molecule on the surface, but rather from migration to a step or defect site on the surface where the threshold energy for dissociation is markedly lower than on the terrace. Seets et al. determined CH_4 dissociative sticking coefficients on Ir(111) on the basis of measurement of the beam fluence required to deposit at least 0.03 monolayer (ML) of C on the surface through CH_4 dissociation. Given that the defect level of the Ir(111) crystal was 0.005 ML, it is expected that any extraordinarily active defect sites would bind C particularly strongly and would be rapidly poisoned such that the influence of defects on the calculated sticking coefficients would be negligible. On this premise, we take the Seets et al. sticking coefficient measurements to be representative of sticking on the Ir(111) terraces alone.

Dynamical steering of the incident molecules by the reactive potential energy surface (PES) toward the minimum energy

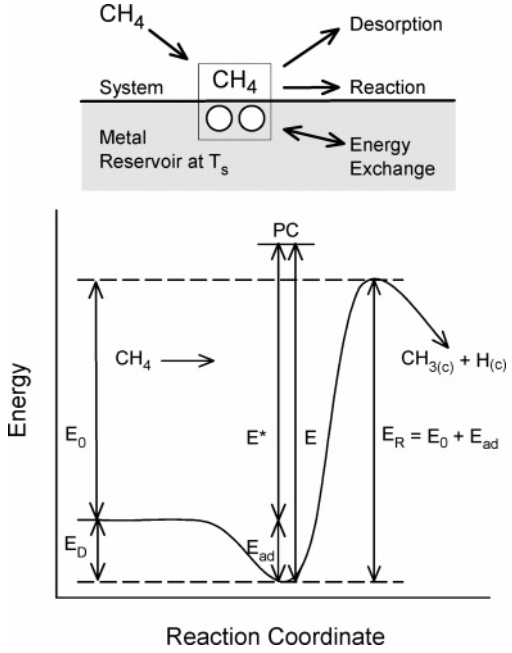

Figure 1. Schematic depiction of the kinetics and energetics of activated dissociative chemisorption. Zero-point energies are implicitly included within the potential energy curve along the reaction coordinate. The energies summing to E are the translational, vibrational, rotational, and adsorption energies of the incident CH_4 and the surface energy of s surface oscillators vibrating at the mean phonon frequency of the substrate.

pathway to products is an effect that might increase the dissociative sticking as the normal translational energy is reduced and relatively more time is spent traversing the region of strong forces.[28] Steering does not produce a V-shaped log S versus E_n curve for the activated dissociation of H_2 on Cu(111)[29] or Cu(100),[30] but steering is claimed to produce this behavior in the nonactivated dissociative chemisorption of H_2 on Pd(100).[28,31] Given that the dissociative chemisorption of CH_4 on Ir(111) is strongly activated and the anisotropy of the reactive PES for dissociation of CH_4 should be less than that for H_2, dynamical steering effects for the CH_4/Ir(111) system are presumed to be negligible.

II. Theoretical Methods

II.A. Physisorbed Complex − Microcanonical Unimolecular Rate Theory (PC-MURT). The PC-MURT assumes the methane dissociative chemisorption kinetics can be microcanonically described as[13]

$$CH_{4(g)} \underset{k_D(E^*)}{\overset{F(E^*)}{\rightleftharpoons}} CH_{4(p)} \xrightarrow{k_R(E^*)} CH_{3(c)} + H_{(c)} \qquad (2)$$

where the E^* zero of energy occurs with methane at infinite separation from the surface when all species are at 0 K (see Figure 1). Methane incident on the surface from the gas phase is assumed to form a transient gas/surface collision complex consisting of a molecule in the neighborhood of the physisorption potential well minimum that interacts with a few immediately adjacent surface atoms. Energy within these collisionally formed physisorbed complexes (PCs) or local hot spots is assumed to become microcanonically randomized in a collision ensemble averaged sense. Diffusion of energy away from the PCs and into the Ir(111) bulk is limited by the ultrafast time scale for desorption at reactive energies and is ignored within the PC-MURT. PCs formed at some total energy E^* can go on to desorb or react dissociatively with the surface to yield chemisorbed fragments with RRKM rate constants $k_D(E^*)$ and $k_R(E^*)$. The steady-state approximation applied to the $CH_{4(p)}$ coverage of eq 2 yields the dissociative sticking coefficient

$$S = \int_0^\infty S(E^*)\, f(E^*)\, dE^* \qquad (3)$$

where

$$S(E^*) = \frac{k_R(E^*)}{k_R(E^*) + k_D(E^*)} = \frac{W_R^{\ddagger}(E^* - E_0)}{W_R^{\ddagger}(E^* - E_0) + W_D^{\ddagger}(E^*)} \qquad (4)$$

is the microcanonical sticking coefficient, $W_i^{\ddagger}$ is the sum of states for transition state i, E_0 is the apparent threshold energy for dissociation, and

$$f(E^*) = \int_0^{E^*} f_t(E_t) \int_0^{E^* - E_t} f_v(E_v) \int_0^{E^* - E_v - E_t} f_r(E_r) \times f_s(E^* - E_t - E_v - E_r)\, dE_r\, dE_v\, dE_t \qquad (5)$$

is the flux distribution for creating a PC at $E^* = E_t + E_v + E_r + E_s$. The $f(E^*)$ is formed by convolution over the various incident CH_4 energy distributions and the surface energy distribution for s oscillators vibrating at the mean Ir phonon frequency, $\nu_s = (^3/_4)k_b\theta_{Debye}/h$, of 215 cm^{-1}. Experimental sticking coefficients are simply predicted via eq 3 by averaging the microcanonical sticking coefficient over the PC flux distribution for the specific experimental conditions.

Noting that the experimental dissociative sticking[9] scales with the normal translational energy alone, $E_n = E_t \cos^2 \vartheta$, we discount parallel molecular translational energy as a spectator or inactive form of energy over the course of the reactive gas−surface collisions and assume that only E_n will contribute to E_t in the expressions above (i.e., set $E_t = E_n$ alone). Following common practice, we further assume that in molecular beam experiments the nozzle temperature, T_n, sets the vibrational and rotational temperatures of the beam molecules as $T_v = T_n$ and $T_r = 0.1\ T_n$, respectively.

The desorption transition state is taken to occur when CH_4 is freely rotating and vibrating in the gas phase, far from the surface. The dissociation transition state is characterized by the nine vibrational modes of CH_4 in the gas, s vibrational modes of the Ir surface oscillators, four vibrational modes at a single lumped frequency ν_D representative of the three frustrated rotations and the vibration along the surface normal of methane at the dissociation transition state, and one of the triply degenerate antisymmetric C−H stretching vibrations ($\nu_3 = 3020$ cm^{-1}) of CH_4 is sacrificed as the reaction coordinate. The resulting PC-MURT has only three adjustable parameters, $\{E_0, \nu_D, s\}$, that can be fixed by comparative simulation to varied experimental data. Dissociative sticking coefficients for a particular set of experiments are simulated using different parameter sets, and the optimal parameter set is considered to be the one that minimizes the average relative discrepancy (ARD)

$$\mathrm{ARD} = \left\langle \frac{|S_{theory} - S_{expt}|}{\min(S_{theory}, S_{expt})} \right\rangle \qquad (6)$$

between the PC-MURT predictions and the experimental sticking. For the CH_4/Ir(111) system, PC-MURT predictions from parameter sets spanning 10 kJ/mol $\le E_0 \le$ 100 kJ/mol, 50 $cm^{-1} \le \nu_D \le$ 250 cm^{-1}, and $1 \le s \le 5$ were compared to selected Seets et al.[9] molecular beam experiments to find the

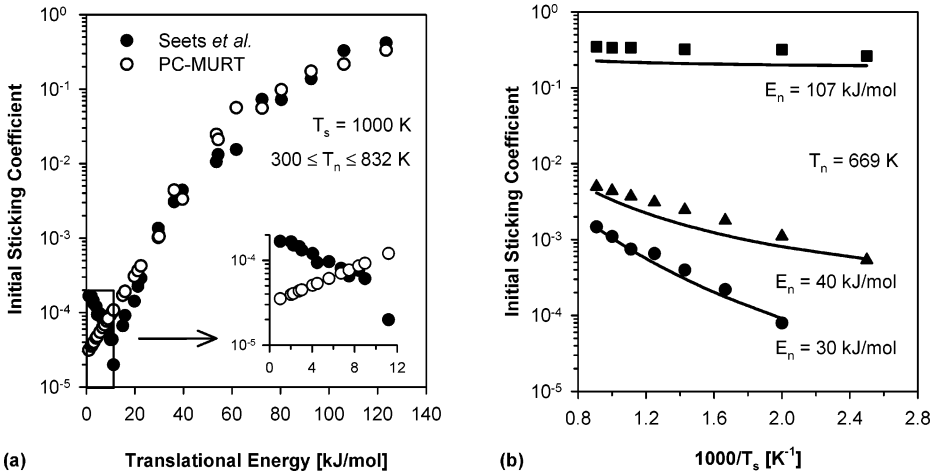

Figure 2. Initial dissociative sticking coefficients for CH_4 on Ir(111) as a function of (a) normal translational energy and (b) surface temperature. Sticking derived from the molecular beam experiments of Seets et al.[9] (closed symbols) are compared to PC-MURT predictions (open symbols and lines) based on parameters $\{E_0 = 39$ kJ/mol, $\nu_D = 185$ cm $^{-1}$, $s = 1\}$.

optimal parameter set of $\{E_0 = 39$ kJ/mol, $\nu_D = 185$ cm^{-1}, $s = 1\}$. This parameter set was used in all further PC-MURT and ME-MURT calculations reported throughout this manuscript.

II.B. Master Equation − Microcanonical Unimolecular Rate Theory (ME-MURT). A master equation (ME) that allows for energy exchange between the PCs formed and the surrounding surface can be written as[13,32]

$$\frac{d\theta_p(E,t)}{dt}dE = F(E,t)\,dE - [k_R(E) + k_D(E)]\theta_p(E,t)\,dE + \int_0^\infty [R(E,E')\,\theta_p(E',t)\,dE - R(E',E)\,\theta_p(E,t)\,dE]\,dE' \quad (7)$$

where $\theta_p(E, t)$ is the coverage distribution of the PCs at energy E, $F(E, t)$ is the external flux distribution that forms PCs at energy E, $k_i(E)$ are RRKM rate constants, pseudo-first-order rate constants of the form $R(E, E')$ govern vibrational energy exchange with the substrate that transfers PCs at energy E' to energy E, and the zero of the E energy scale is at the bottom of the physisorption well such that $E = E^* + E_{ad}$ (see Figure 1). Typically, in gas-phase energy exchange involving bimolecular collisions, $R(E, E')$ is written as the product of an inelastic collision frequency, ω, and a collision step size distribution, $P(E, E')$, so that $R(E, E') = \omega \cdot P(E, E')$.[33] On the surface, vibrational energy exchange will be mediated by phonons and the maximum value of ω is likely to be about three times the mean Ir phonon frequency ($\nu_s = 6.45 \times 10^{12}$ Hz; 215 cm^{-1}), because phonons can bathe the PCs from three independent directions. Once the downward energy transfer for $P(E, E')$ is prescribed, the upward energy transfer is fixed by detailed balance. In this manuscript, a downward energy transfer of about 10% of the surface ergodic collision theory[32,34,35] (SECT) $P(E, E')$ predictions is applied to define reasonable parameters for a Lenzer et al.[36] generalized exponential down model of $P(E, E')$. These SECT and Lenzer labeled $P(E, E')$s define energy exchange via ergodic mixing and a more realistic semi-empirically derived estimate, respectively. With the $R(E, E') = \omega \cdot P(E, E')$ form of the energy exchange, eq 7 can be written as

$$\frac{d\theta_p(E,t)}{dt} = F(E,t) - [k_R(E) + k_D(E) + \omega]\theta_p(E,t) + \omega\int_0^\infty P(E,E')\,\theta_p(E',t)\,dE' \quad (8)$$

and solved numerically using matrix methods.[13,32] When a time-independent flux of gas is made incident on the surface according to $F(E, t) = F_0\, f(E)$, the steady-state approximation applied to the $\theta_p(E, t)$ coverage distribution of eq 8 yields the sticking coefficient

$$S = \frac{1}{F_0}\frac{d\theta_c}{dt} = \frac{1}{F_0}\int_0^\infty k_R(E)\,\theta_p^{ss}(E)\,dE \quad (9)$$

where θ_c is the chemisorbed coverage of either of the dissociation fragments of the eq 2 kinetics. A formal solution for the steady-state PC distribution of eq 8 is

$$\theta_p^{ss}(E) = \frac{F_0 f(E) + \omega\int_0^\infty P(E,E')\,\theta_p^{ss}(E')\,dE'}{k_R(E) + k_D(E) + \omega} \quad (10)$$

which illustrates that $\theta_p^{ss}(E)$ is governed by the external flux and energy transfer source terms and decays via reaction, desorption, and energy transfer. In the limit that energy exchange between the surface and PCs vanishes (e.g., $\omega \rightarrow 0$), eq 8 simplifies to define the PC-MURT kinetics and eq 9 evolves into eq 3. A canonical thermal distribution for $\theta_p^{ss}(E)$ is obtained in the infinite inelastic collision frequency strong collision (IFSC) approximation where it is assumed that the collision step size distribution is the canonical thermal distribution for the PCs, $P(E, E') = B(E; T)$, (i.e., the strong collision approximation (SCA) of gas-phase kinetics)[37] and the collision frequency ω is made sufficiently (∼infinitely) high. The high ω and SCA of the IFSC approximation are able to overwhelm the desorptive and reactive loss of PCs at high energies and ensure that a thermal steady-state PC population can be maintained. Gas-phase studies have shown that the SCA, though a mathematically useful approximation, is not especially realistic, and collisionally mediated vibrational energy transfer is usually considerably weaker.[33,37] It should be noted that the thermal-trapping-mediated sticking mechanism[8] of eq 1 assumes that the IFSC limit is reached for the ζ fraction of the incident methane that becomes trapped.

III. Results and Discussion

III.A. Comparison of Experiments and PC-MURT. Figure 2 compares dissociative sticking coefficients for CH_4 on Ir(111) derived from the molecular beam experiments of Seets et al.[9] with the predictions of the PC-MURT. The $\{E_0 = 39$ kJ/mol,

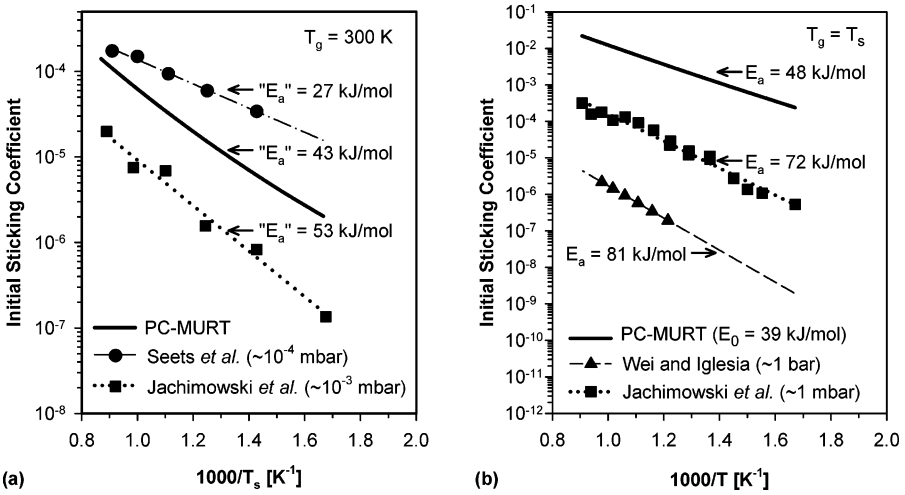

Figure 3. Intermediate pressure experimental sticking (points) for CH_4 on Ir(111)[9,10] and supported Ir nanocrystallite catalysts,[6,7] along with their Arrhenius sticking extrapolations (dashed lines), are compared to PC-MURT predictions (solid lines). Effective activation energies "E_a"'s obtained under nonequilibrium conditions (i.e., $T_g = 300$ K and $T_s \approx 800$ K) and activation energies E_a's obtained under thermal equilibrium conditions at $T \approx 800$ K are given.

$\nu_D = 185$ cm^{-1}, $s = 1$} parameter set was found to minimize the ARD between the PC-MURT predictions and the sticking derived from experiments with $E_n \geq 10$ kJ/mol, which includes all the molecular beam experiments in which methane was seeded in either He or H_2. The overall ARD for Figure 2 is 88% (55% for the $E_n \geq 10$ kJ/mol sticking). All subsequent PC-MURT and ME-MURT sticking predictions were made using the optimized parameter set above. Figure 2a depicts the dissociative sticking as a function of normal translational energy over a 1000 K surface. The inset of Figure 2a provides a closer look at the divergence between the PC-MURT sticking predictions and the sticking measured at $E_n < 10$ kJ/mol using anti-seeded (i.e., CH_4 slowed in primarily Ar or Kr) molecular beams. The ARD for the optimized sticking of Figure 2a with $E_n \geq 10$ kJ/mol (i.e., CH_4 seeded in He or H_2) is 78%, and by including the sticking at lower E_n, the overall ARD for Figure 2a rises to 123%. The dependence of the dissociative sticking on surface temperature at several E_n above 10 kJ/mol is predicted in Figure 2b with an ARD of just 34%. Except for the upturn in the dissociative sticking at $E_n < 10$ kJ/mol, the PC-MURT describes the Figure 2 molecular beam data quite well.

Figure 3 illustrates varied dissociative sticking measurements and PC-MURT predictions for intermediate pressures of CH_4 incident on Ir(111) and supported Ir catalyst under both nonequilibrium and equilibrium conditions. Arrhenius fits to the nonequilibrium sticking of Figure 3a in which a 300 K gas impinges on a variable-temperature surface yield effective activation energies "E_a"'s of 27 ± 4 kJ/mol for the Seets et al.[9] data and 53 kJ/mol for the Jachimowski et al.[10] data. The PC-MURT predicts an effective activation energy of "E_a" = 43 kJ/mol, which is intermediate between these values. In Figure 3b, Arrhenius analysis of the thermal equilibrium sticking measured by Jachimowski et al.[10] on Ir(111) and Wei and Iglesia[6,7] on supported Ir catalysts yields $E_a = 72$ kJ/mol and $E_a = 81$ kJ/mol, respectively. These activation energies are significantly higher than the PC-MURT prediction for Ir(111) of $E_a = 48$ kJ/mol. It is noteworthy that the Seets et al. $T_g = 300$ K gas experiments of Figure 3a, that are characterized by methane mean normal translational energies of $\langle E_n \rangle \approx k_b T_g \approx 2.5$ kJ/mol, have sticking coefficients that are consistently higher than the PC-MURT predictions, just as the Seets et al. molecular beam experiments of Figure 2a are at low translational energies near $E_n = 2.5$ kJ/mol. These observations are consistent with the trapping-mediated sticking significantly augmenting the direct sticking at low E_n.

The thermal dissociative sticking coefficient for 0.8 wt. % Ir/ZrO_2 supported catalyst was derived from Wei and Iglesia's[6,7] measurements of catalyst initial turnover rates for methane decomposition over the catalyst at 1 bar (20 kPa CH_4 and 80 kPa Ar) pressure at temperatures from 823 to 1023 K, where the rate could be described by

$$r = k(T)\, P_{CH_4} = (k_0\, e^{-E_a/RT}) P_{CH_4} \qquad (11)$$

where r is the turnover rate per surface exposed Ir atom, $k(T)$ is an Arrhenius rate constant, and P_{CH_4} is the partial pressure of methane gas. Wei and Iglesia[6,7] report a turnover rate of 11.2 s^{-1} at 873 K, a preexponential factor of $k_0 = 39.3$ s^{-1} Pa^{-1}, and an activation energy of $E_a = 81 \pm 6$ kJ/mol. The initial turnover rate per exposed Ir atom on the catalyst surface was converted into an equivalent initial sticking coefficient on Ir(111) (i.e., as if the catalyst exposed only Ir(111) nanofacets) using the relation

$$r = k(T)\, P_{CH_4} = N_s^{-1} \frac{d\theta_c}{dt} = N_s^{-1} SF \qquad (12)$$

where N_s is the 1.57×10^{19} m^{-2} areal density of surface atoms on Ir(111), θ_c is the coverage of either of the chemisorbed fragments in the eq 2 dissociation kinetics, S is the initial sticking coefficient, and F is the thermal flux of methane gas impinging on the surface. The final expression for the equivalent sticking coefficient on Ir(111) is

$$S = k_0\, e^{-E_a/RT} N_s \sqrt{2\pi m k_b T} \qquad (13)$$

which is plotted in Figure 3b. Impressively, the CH_4 dissociative sticking coefficient on the supported Ir catalyst is some 4 orders of magnitude less than the PC-MURT prediction for sticking on the Ir(111) surface.

As illustrated by Figure 3, there is little agreement between the activation energies and absolute values of the sticking coefficients obtained by the various experimentalists and PC-MURT calculations for methane dissociative chemisorption on Ir(111). The PC-MURT prediction for "E_a" under thermal nonequilibrium conditions is within the experimental range

observed, varying from each by ~12 kJ/mol. However, the PC-MURT predicted activation energy shown in Figure 3b is substantially lower than the experimental values, differing by ~30 kJ/mol. PC-MURT predicts a reaction threshold energy of $E_0 = 39$ kJ/mol, almost halfway between the theoretical values obtained from DFT calculations (i.e., 15 ± 10 kJ/mol[11] and 76 kJ/mol[12]). Interestingly, the unusual transition state proposed by Henkelman and Jónsson[11] in which a single iridium atom rises from the surface by ~0.4 Å seems to correlate with the PC-MURT's single surface oscillator parameter (i.e., $s = 1$) for CH_4/Ir(111), which compares to $s = 2$ for CH_4/Ni(100)[18] and $s = 3$ for CH_4/Pt(111).[13] The surface degrees of freedom clearly participate in the dissociative chemisorption as evidenced by the surface temperature dependence of the sticking exhibited in Figure 2b.

Although it is disconcerting that the two sets of experiments illustrated in Figure 3a and performed under essentially identical conditions differ in the absolute value of their sticking coefficients by roughly 2 orders of magnitude, considerable variance in sticking results derived from different laboratories is not uncommon for these difficult measurements.[1,17] We are inclined to believe that the Seets et al. results are more accurate than the Jackimowski et al. results because the Seets sticking values are based on Auger measurements of C deposited after defined methane exposures that were cross-correlated with King and Wells[38] sticking measurements at higher exposures. The Jackimowski et al. sticking coefficients were made without the benefit of Auger spectroscopy or other surface elemental analysis techniques associated with their ultrahigh-vacuum chamber and were derived solely on the basis of mass spectrometric measurements of CO_2 produced by oxidation of the adsorbed C that was deposited by varied CH_4 exposures. If we assume that the Jackimowski et al. results differ from those of Seets et al. by only a systematic multiplicative calibration factor of ~100, then the Jackimowski et al. thermal sticking of Figure 3b falls fairly close to, but still mostly below, the thermal sticking values predicted by the PC-MURT. A further complication is that the Jackimowski et al. thermal sticking experiments of Figure 3b were performed by impingement of a 300 K gas at a pressure of 1.33 mbar under the assumption that the short mean free path of gas at this pressure would serve to produce an impinging gas layer above the surface that would be in thermal equilibrium with the hot surface. Chorkendorff and co-workers[1] have shown that complete thermalization of methane to the surface temperature in such thermal bulb experiments may require slightly higher pressures (i.e., ≥ 3 mbar) or the presence of a thermal finger in front of the reactive surface to fully equilibrate the gas. Certainly, Jackimowski et al. observed roughly 1 order of magnitude increase in the dissociative sticking coefficient as the gas pressure was raised from 10^{-3} mbar to 1 mbar in going from the Figure 3a to Figure 3b experiments (n.b., the PC-MURT predicts a ~100-fold increase), but even Jackimowski et al. expressed doubt that the molecular vibrational temperature was fully accommodated to the surface temperature at the elevated 1 mbar pressure. In summary, the PC-MURT sticking predictions are consistently lower than the values measured by Seets et al. for the 300 K gas experiments and are somewhat greater than the values measured by Jackimowski et al. for thermal sticking.

A surprising finding illustrated graphically in Figure 3b is that the PC-MURT predicts a thermal dissociative sticking coefficient for CH_4 on Ir(111) some 4 orders of magnitude greater than the thermal sticking per exposed Ir atom observed for 0.8 wt. % Ir/ZrO_2 supported catalyst. This is unexpected because (i) the catalyst sticking derived through eq 11 represents an upper bound, because the Ir(111) N_s employed is the maximum for any Ir crystalline surface and the real catalyst likely exposes a number of different facets, some with lesser N_s, and (ii) Wei and Iglesia found that the CH_4/Ir sticking is structure sensitive and increases with increasing catalyst dispersion.[5] The fractional dispersion of the 0.8 wt. % Ir/ZrO_2 supported catalyst was measured[6] as $D = 0.52$, which yields an average Ir nanocrystallite diameter of $1/D$ nm ≈ 2 nm. At this relatively high dispersion, the catalyst should expose considerable numbers of steps, kinks, and adatoms, or equivalently, higher-index surface planes with less coordinatively saturated sites. In consequence, the nanoscale Ir catalyst would normally be expected to display a reactivity considerably higher than that of the flat Ir(111) surface. The much higher dissociative sticking coefficient predicted for the Ir(111) surface suggests that the working catalyst may be poisoned in some way (e.g., by dissolved C) under working conditions. Figure 3b is suggestive that substantial improvements in catalyst turnover rates might be possible to achieve for different Ir catalyst formulations.

As discussed briefly above, the unusual V-shaped log S versus E_n dissociative sticking curve observed in Figure 2a for CH_4/Ir(111) has been postulated to result from parallel direct and thermal-trapping-mediated reaction mechanisms.[9] Assuming that the PC-MURT analysis of the molecular beam sticking at $E_n >$ 10 kJ/mol defines the direct reaction mechanism, it is possible to provide an approximate estimate for the thermal trapping coefficient within eq 1

$$S_{expt} = S_{trap} + S_{direct} = \zeta(E, \vartheta; T_s)\frac{k_R(T_s)}{k_R(T_s) + k_D(T_s)} + S \simeq \zeta\left\langle \frac{k_R(E^*)}{k_R(E^*) + k_D(E^*)} \right\rangle_{T=T_s} + S$$

$$\simeq \zeta \int_0^\infty S(E^*)\, f_T(E^*)\, dE^* + S = \zeta S_T + S \quad (14)$$

$$\zeta \simeq \frac{S_{expt} - S}{S_T} \quad (15)$$

with the aid of eqs 3−5 where the thermal average over the competitive reaction and desorption rate constants can be written as the average of the microcanonical sticking coefficient, $S(E^*)$, over the thermal PC flux distribution, $f_T(E^*)$, to yield the PC-MURT thermal sticking coefficient, S_T. The thermal trapping mechanism apparently dominates the sticking at low E_n, and it is interesting to compare the ratio of the Seets et al.[9] experimental sticking coefficient to the PC-MURT sticking coefficient, S_{expt}/S, at particular E_n, T_g, and T_s values. In the molecular beam experiment of Figure 2a at $E_n = 2.5$ kJ/mol (i.e., $E_n/k_b = T_t \approx$ 300 K) with a nozzle temperature of 300 K and $T_s = 1000$ K, the sticking ratio is $S_{expt}/S = 3.9$. This ratio is similar to the $S_{expt}/S = 2.4$ value for the nonequilibrium experiment with $T_g = 300$ K and $T_s = 1000$ K of Figure 3a. Thus, the low E_n sticking enhancement is consistently observed in both the molecular beam experiments and the nonequilibrium ambient gas experiments at low T_g. This finding provides assurance that the Seets et al. change in molecular beam seeding procedures to anti-seeding in Ar or Kr for $E_n \leq 10$ kJ/mol is not responsible for somehow increasing the measured sticking at low E_n. Estimates of the thermal trapping coefficient at $T_s = 1000$ K and $T_g \approx 300$ K from eq 15 are $\zeta = 0.0090$ and $\zeta = 0.0071$

TABLE 1: Mean Energies Derived from the *j*th Reactant Degrees of Freedom for All Physisorbed Complexes (PCs) $\langle E_j \rangle$ and for Successfully Reacting PCs $\langle E_j \rangle_R$ and Differential Energy Uptakes d_j for Various Experiments at $T_s = 1000$ K According to the PC-MURT

	molecular beam $T_n = 300$ K, $T_t = 10$ K			thermal nonequilibrium $T_g = 300$ K			thermal equilibrium $T_g = T_s$		
mode (*j*)	$\langle E_j \rangle$ kJ/mol	$\langle E_j \rangle_R$ kJ/mol	d_j %	$\langle E_j \rangle$ kJ/mol	$E_j \rangle_R$ kJ/mol	d_j %	$\langle E_j \rangle$ kJ/mol	$\langle E_j \rangle_R$ kJ/mol	d_j %
translation (t)	2.5	2.55	0.08	2.5	3.6	2.0	8.3	14.0	11.0
vibration (v)	0.1	0.9	1.3	0.1	0.9	1.4	15.0	46.5	61.4
rotation (r)	0.37	0.38	0.02	3.7	5.3	3.0	12.5	20.9	16.6
surface (s)	7.1	63.0	98.6	7.1	57.0	93.6	7.1	12.7	11.0
sum	10.1	66.8	100	13.4	66.8	100	42.9	94.1	100
sticking coefficient		3.71×10^{-5}			6.24×10^{-4}			1.23×10^{-2}	

based on the molecular beam and nonequilibrium bulb experiments, respectively. These trapping coefficients are 1−2 orders of magnitude smaller than those suggested by Mullins and Sitz's[22] trajectory calculations and by Jackomowski et al. If the trapping coefficient is actually greater than 0.01, then the PC-MURT indicates that the trapped molecules cannot all be completely thermalized to the surface temperature.

III.B. Energy Uptake and Availability in Low E_n Experiments. For the direct sticking mechanism, the PC-MURT provides a formalism to characterize how the different degrees of freedom contribute toward the energy required to surmount the activation barrier for dissociative chemisorption. Differential energy uptakes are usefully defined as

$$d_j \equiv \frac{\langle E_j \rangle_R - \langle E_j \rangle}{\langle E^* \rangle_R - \langle E^* \rangle} \tag{16}$$

where $\langle E_j \rangle_R$ is the mean energy derived from the *j*th reactant degree of freedom for those PCs that successfully react, $\langle E_j \rangle$ is the mean energy derived from the *j*th reactant degree of freedom for all PCs, $\langle E^* \rangle_R$ is the mean total energy for those PCs that successfully react, and $\langle E^* \rangle$ is the mean total energy for all PCs where the averages are appropriate to the specific experimental conditions. As derived elsewhere,[13] under thermal equilibrium conditions, the activation energy is

$$E_a(T) \equiv -k_b \frac{\partial \ln S}{\partial\left(\frac{1}{T}\right)} = \langle E^* \rangle_R - \langle E^* \rangle \tag{17}$$

Under any conditions where the *j*th reactant degree of freedom is described by a canonical thermal distribution, an effective activation energy for the *j*th degree of freedom is[13]

$$\text{“}E_a\text{”}(T_j) \equiv -k_b \frac{\partial \ln S}{\partial\left(\frac{1}{T_j}\right)} = \langle E_j \rangle_R - \langle E_j \rangle \tag{18}$$

As can be seen from the nonequilibrium Arrhenius plots of Figures 2b and 3a, “E_a” values depend very much on the experimental particulars and are not trivially related to the reaction threshold energy, E_0, that is diagnostic of the reactive transition state. Under thermal equilibrium conditions

$$d_j = \frac{\text{“}E_a\text{”}(T_j)}{E_a(T)} \tag{19}$$

and under any experimental conditions the d_js sum to 1.

Table 1 lists PC-MURT calculations for $\langle E_j \rangle$, $\langle E_j \rangle_R$, and d_j for several different kinds of experiments at a surface temperature of 1000 K. Differential energy uptakes for the nonequilibrium experiments show that the preponderance of energy required to overcome the activation barrier to reaction derives from the surface, ∼96%. In contrast, under thermal equilibrium conditions, 89% of the activation energy derives from the molecular degrees of freedom. The PC-MURT is a statistical theory that treats all kinds of energy equivalently, and so, only the relative availability of energy from the different reactant degrees of freedom can be important in determining the differential energy uptakes. The surface energy reservoir is the most flexible one in the nonequilibrium experiments, because the exponential Boltzmann damping of the constituent canonical distributions is far less severe at the relatively high surface temperature ($T_s = 1000$ K) than at the much lower temperatures of the other degrees of freedom, ($T_{j \neq s} \leq 300$ K). At thermal equilibrium, all degrees of freedom share a common temperature and the Boltzmann damping is the same. Consequently, at thermal equilibrium, it is the density of states of the different reactant degrees of freedom that determines the relative availability of energy from the different energy reservoirs.

The E^* energy sums of Table 1 illustrate that a parallel thermal trapping mechanism would need to heat the initially trapped PCs of the molecular beam experiment considerably in order to thermalize them to T_s and subsequently dissociate them with the thermal sticking probability of the PC-MURT. Establishing and maintaining a thermal distribution of PCs after trapping such that the average energy of the thermally reacting PCs is 94.1 kJ/mol above the desorption energy (n.b., E_D is at $E^* = 0$; see Figure 1) is unlikely to be sustainable, as will be shown more explicitly in ME-MURT simulations below.

III.C. Energy Transfer and Trapping. Figure 4 contrasts ME-MURT and PC-MURT simulations of the Seets et al.[9] molecular beam experiments of Figure 2a performed at $T_s = 1000$ K. In the IFSC approximation, PCs formed are immediately thermalized to the surface temperature, and the ME-MURT returns the thermal sticking coefficient independent of the initial energy of the incident methane. The thermal equilibrium sticking coefficient predicted by the PC-MURT is shown for comparison. Clearly, the IFSC overestimates the energy transfer, because the experimental sticking varies with methane translational energy. As discussed briefly in section II.B, the collision step size distribution, $P(E, E')$, in the SECT is based on ergodic mixing of the energy of the surface oscillator and the other degrees of freedom of the PC in such a way that the PC's surface oscillator resamples the surface Boltzmann distribution upon every inelastic phononic collision. Although the SECT energy transfer model is more physically motivated than the IFSC, it still only provides an approximate upper bound for what the energy transfer at the surface might be. In studies of gas-phase bimolecular collisions, Nordholm and co-workers[35] have shown that a partially ergodic collision theory (PECT)

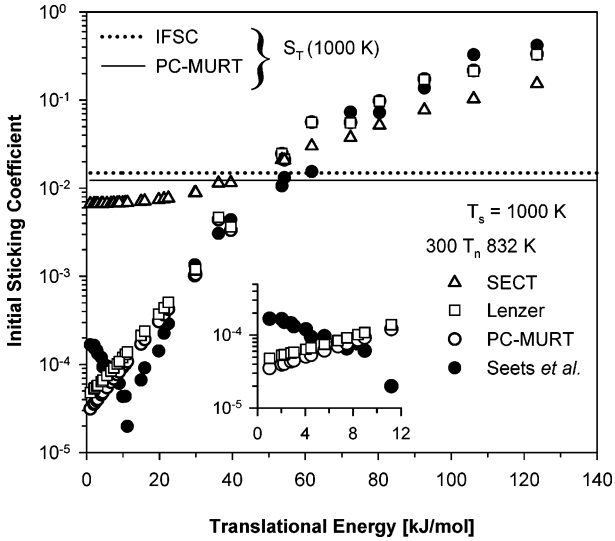

Figure 4. ME- and PC-MURT calculations for the Seets et al.[9] molecular beam experiments of Figure 2a are compared. The ME-MURT calculations employ different collision step size distributions in modeling the physisorbed complex/surface vibrational energy transfer: the infinite frequency strong collision (IFSC) approximation is for strong phononic collisions in the $\omega \rightarrow \infty$ limit, surface ergodic collision theory (SECT) provides an upper bound for energy transfer in weak collisions, and the Lenzer model provides a more realistic estimate for weak collisions (see text for details).[32] The SECT and Lenzer ME-MURT calculations employed an inelastic collision frequency of $\omega = 6 \times 10^{12}$ s^{-1}.

agrees well with Lenzer and co-workers'[36] experimentally optimized generalized exponential down $P(E, E')$ when the PECT is constructed with a reduced number of active modes to recover roughly 10% of the ergodic collision theory (ECT)[34] energy transfer. Nordholm's procedure is attractive, because the ECT and PECT (arguably) employ no adjustable parameters and thereby require no prior, system dependent, experimental knowledge. Here, we used 10% of the downward energy transfer predicted by the SECT to choose parameters for a density of states weighted exponential down model for the $P(E, E')$

$$P(E, E') = \frac{\rho(E)}{N(E')} \exp\left(-\left|\frac{E' - E}{c_0 + c_1 E'}\right|^{\gamma}\right) \qquad (20)$$

of the Lenzer style leading to $c_0 = 195$ cm^{-1}, $c_1 = 0.30$, and $\gamma = 1$. The inelastic phononic collision frequency ω of the eq 8 master equation was chosen by minimizing the ARD for the ME-MURT sticking simulations of the Seets et al. molecular beam experiments of Figure 4 using the "Lenzer" $P(E, E')$ of eq 20. A frequency of $\omega = 6 \times 10^{12}$ s^{-1} (cf., mean Ir phonon frequency $\nu_s = 6.45 \times 10^{12}$ s^{-1}) minimized the ME-MURT ARD at 114%, which gave only a modest improvement over the PC-MURT ARD of 123% for these experiments. The same ω was used in both the Lenzer and SECT simulations of Figure 4. Comparisons to experiment indicate that the SECT overestimates the energy transfer, whereas the Lenzer energy transfer only modestly improves upon the PC-MURT. None of the energy transfer models provide any evidence for a "V" in the sticking simulation curves near $E_n = 10$ kJ/mol.

Figure 5 compares the steady-state coverage for physisorbed complexes, $\theta_p^{ss}(E)$, for several different energy transfer models in ME-MURT simulations of an $E_n = 10$ kJ/mol molecular beam experiment. Both the Lenzer and PC-MURT $\theta_p^{ss}(E)$ distributions have quite similar high-energy tails that damp down much sooner than the thermal distribution of the IFSC. The PC-MURT

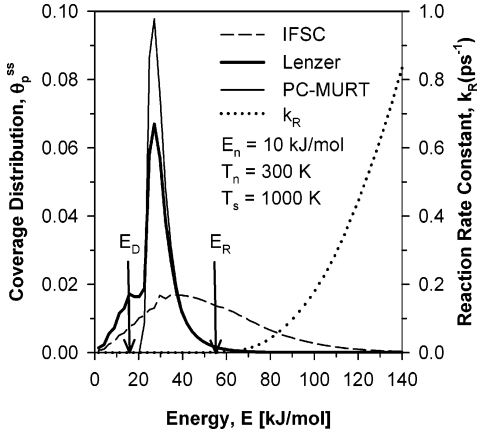

Figure 5. Steady-state coverage distributions for physisorbed complexes, $\theta_p^{ss}(E)$, are illustrated for several different energy transfer models for a particular molecular beam experiment. The RRKM reaction rate constant is also shown whereby the dissociative sticking may be calculated as $S = 1/F_0 \int_0^{\infty} k_R(E)\theta_p^{ss}(E)\, dE$.

provides for no energy transfer with the surrounding surface, and because all PCs gain the adsorption energy during their formation, its $\theta_p^{ss}(E) = F_0\, f(E)/[k_R(E) + k_D(E)]$ has no population at energies below $E = E_{ad} = E_D$, or $E^* = 0$. The ME-MURT simulation with the more physically realistic Lenzer energy transfer model shows that some PCs become trapped in the physisorption well (i.e., with $E < E_D$), but energy transfer rates are insufficient to sustain a thermal distribution at reactive energies (i.e., $E \geq E_R$) in the face of competitive desorption and reaction. This is an important result in that it illustrates that trapped molecules are unlikely to become completely thermalized to the full IFSC limit. Consequently, the assumption within the thermal-trapping-mediated sticking mechanism of eq 1 that trapped molecules will be thermalized to the full IFSC limit is likely untenable when $E_R \gg E_D$. For such nonequilibrium sticking, the parameters of eq 1 cannot be confidently interpreted in typical Arrhenius fashion (cf., "E_a" of eq 18 and Figure 2b) to provide definitive information about the transition-state characteristics of the reactive PES.

Although we have failed to quantitatively explain the trapping-mediated/energy transfer sticking observed by Seets et al. for CH_4/Ir(111) at high T_s, this sticking channel is robustly observable under several different nonequilibrium conditions. PC-MURT-based estimates of the trapping coefficient ζ based on eq 15 suggest an effective $\zeta \approx 0.01$. Assuming that on other flat surfaces this same trapped fraction of the molecular beam flux sticks with the PC-MURT thermal sticking coefficient at low E_n, thermal trapping would have raised the sticking coefficient of earlier beam experiments for (i) CH_4 on Pt(111)[39] at $T_s = 800$ K by $\Delta S = 8 \times 10^{-6}$ and (ii) CH_4 on Ni(100)[40] at $T_s = 475$ K by $\Delta S = 4 \times 10^{-10}$, which would have been below detectable levels. The relatively high 1000 K surface temperature coupled with the low threshold energy for dissociative chemisorption and low E_n of the Seets et al. experiments apparently combine to make the trapping/energy transfer mediated sticking more readily observable for the CH_4/Ir(111) system.

An interesting question raised by Seets et al. is, "Will the direct or trapping mediated sticking channel dominate the thermal sticking?" At thermal equilibrium, the PCs of the PC-MURT direct channel will be microcanonically trapped as usual, but will be formed in quasi-thermal equilibrium with the surface (e.g., eq 5) such that the PC-MURT channel becomes a kind of thermalized trapping channel with $\zeta = 1$ for $E^* \geq E_0$. For the PCs formed at $E^* < E_0$, upward energy transfer processes to

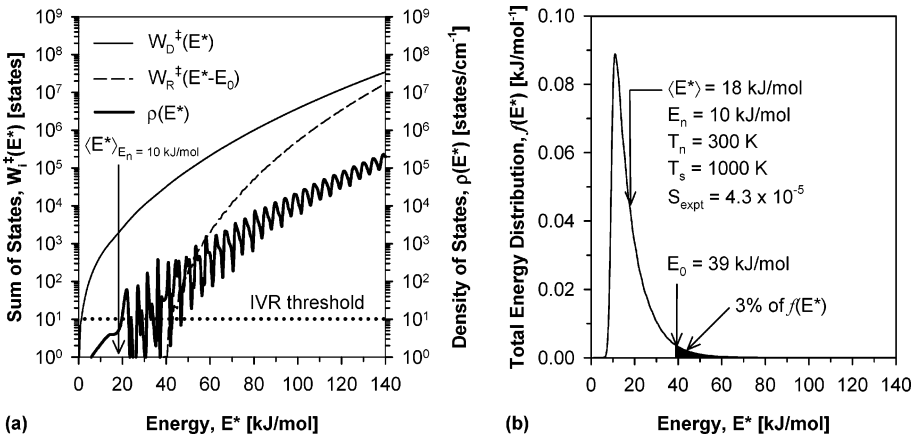

Figure 6. (a) The sum of states for desorption $W_D^{\ddagger}(E^*)$ and reaction $W_R^{\ddagger}(E^* - E_0)$ are shown with the density of states for the physisorbed complex $\rho(E^*)$. The density of states intersects the typical IVR threshold density of ~10 states/cm^{-1} close to $\langle E^* \rangle = 18$ kJ/mol mean energy for a molecular beam experiment under Figure 2a conditions at $E_n = 10$ kJ/mol. (b) The physisorbed complex energy distribution $f(E^*)$ for a molecular beam experiment at $E_n = 10$ kJ/mol, $T_n = 300$ K, and $T_s = 1000$ K appropriate to Figure 2a. As illustrated, only 3% of the physisorbed complexes formed have enough energy to overcome the reaction threshold energy $E_0 = 39$ kJ/mol for dissociation.

$E^* \geq E_0$ should be balanced by complementary downward processes under thermal equilibrium such that the net energy transfer between gas and surface ceases. Accordingly, the thermal sticking is expected to be dominated by the PC-MURT direct sticking channel. No separate accounting of other parallel energy transfer mediated sticking is necessary, because these will sum to zero in the IFSC limit (n.b., for which the integrand of eq 7 vanishes by detailed balance) that the PC-MURT approximates at thermal equilibrium.[32]

III.D. IVR Threshold and Dynamical Trapping. Figure 6a illustrates how the PC density of states, $\rho(E^*)$, and desorption and reactive sums of states, $W_i^{\ddagger}(E^*)$, vary as a function of energy. Figure 6b shows the $f(E^*)$ flux distribution for forming a PC at energy E^* under the molecular beam conditions of Figure 2a at $E_n = 10$ kJ/mol. The mean energy of the PCs created in this beam experiment, $\langle E^* \rangle = 18$ kJ/mol, is very close to the energy where the PC density of states exceeds 10 states/cm^{-1}, the typical threshold density of states required for IVR in gas-phase molecules.[41,42] We speculate that just as exceeding the energy of the IVR threshold density of states signals a change in the vibrational dynamics of polyatomic gas-phase molecules it may be that crossing the IVR threshold energy, E^*_{IVR}, (e.g., where $\rho(E^*_{IVR}) = 10$ states/cm^{-1}) signals a qualitative change in the PC vibrational dynamics at the surface. Such behavior might help explain the abrupt change in the CH_4/Ir sticking behavior near $E_n \approx 10$ kJ/mol in Figure 2a. At energies above the IVR threshold, statistical theories of the surface reaction kinetics and energy transfer are more likely to successfully apply, whereas below the IVR threshold, a dynamical treatment of the kinetics is probably necessary.

Figure 6b is instructive in discussion of how the direct PC-MURT sticking might work in concert with a parallel dynamical trapping pathway. The key assumption in the PC-MURT is that energy in the possibly reactive PCs formed with $E^* \geq E_0$ becomes microcanonically redistributed in a collision ensemble-averaged sense either by the collisions themselves or by rapid IVR, or both. Anharmonic mode couplings near the transition state on the distorted PES for CH_4 dissociation on Ir(111) are likely high and conducive to IVR, because the threshold energy for CH_4 dissociation is substantially reduced from $E_0 = 438$ kJ/mol in the gas phase to 39 kJ/mol on the surface. The PC-MURT provides no direct information about PCs formed at $E^* < E_0$, and certainly as the energy is lowered, IVR will eventually turn off, and the CH_4 scattering dynamics will increasingly resemble those of Ne. The $P(E, E')$s used in the ME-MURT simulations are statistically based and should perform best at energies above the IVR threshold. No evidence of the sharply V-shaped log S versus E_n experimental behavior near $E_n = 10$ kJ/mol was observed in the ME-MURT simulations. It may be that at the IVR threshold energy the CH_4/Ir(111) vibrational energy transfer dynamics change fairly abruptly (a behavior that our statistical models do not explicitly predict). Certainly, any low-energy dynamical trapping/energy transfer events that are able to transfer PCs formed at energies below E_0 to above E_0 would contribute to a dynamical sticking channel parallel to the PC-MURT direct channel. Nevertheless, as discussed above, net energy transfer processes should cease at thermal equilibrium, and the thermal sticking should be dominated by the PC-MURT direct sticking.

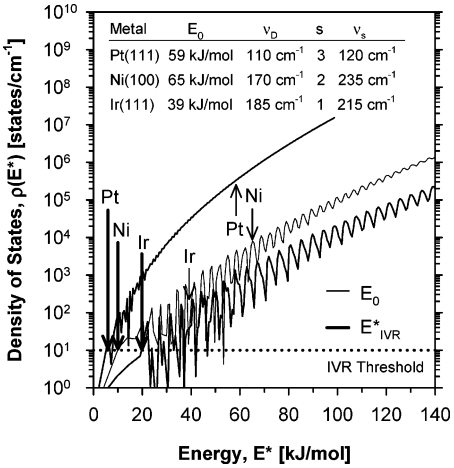

Figure 7. Comparison of physisorbed complex density of states, PC-MURT parameters, and mean metal phonon frequencies, ν_s's, for CH_4 on Ir(111), Ni(100),[18] and Pt(111).[13] Estimated threshold energies for IVR, E^*_{IVR}, based on $\rho(E^*_{IVR}) = 10$ states/cm^{-1}, and reaction threshold energies, E_0's, are marked by arrows.

Figure 7 compares the PC density of states and estimated threshold energies for IVR for several CH_4 dissociative chemisorption systems. The density of state counts are lower bounds, because they assume the PCs have the same lumped low frequency, ν_D, for the three frustrated rotations and normal vibrational mode that was derived for the reactive transition

state on the different surfaces, whereas for methane in the physisorption well these mode frequencies are likely to be somewhat lower. Figure 7 is suggestive that the CH_4/Ir dissociative chemisorption system should be the most likely one to display observable dynamical (nonstatistical) behavior, because its density of states is relatively low and its E^*_{IVR} is highest.

IV. Summary

Nonequilibrium molecular beam experiments probing the dependence of the dissociative sticking coefficient, S, for CH_4 on Ir(111) as a function of normal translational energy, E_n, and surface temperature were reasonably well-described (i.e., ARD = 88%) by the PC-MURT with three parameters: $\{E_0 = 39$ kJ/mol, $\nu_D = 185$ cm^{-1}, $s = 1\}$. The upturn in the molecular beam S as E_n was decreased below ~10 kJ/mol was not reproduced in PC-MURT simulations. ME-MURT simulations with a fairly realistic phononic energy transfer model also failed to reproduce the upturn in the sticking at low E_n. However, the ME-MURT simulations did establish that a trapping/energy transfer process in which the surface heats the trapped methane is unlikely to fully thermalize the molecules. It was suggested that the central "complete thermalization" tenet of the thermal-trapping-mediated sticking model will fail for highly activated sticking. Although the trapping/energy transfer mediated sticking was observable in the nonequilibrium molecular beam experiments at low E_n, it was argued that this trapping channel should be a minor contributor to the thermal sticking under equilibrium conditions. It was noted that the mean energy of the PCs formed at the onset of the trapping-mediated sticking (i.e., at $E_n \approx 10$ kJ/mol) coincides with the estimated threshold energy for intramolecular vibrational energy redistribution, E^*_{IVR}, within the PCs. It was speculated that crossing the IVR threshold energy might produce a relatively abrupt change in the phononic energy transfer dynamics and hence might help qualitatively explain the V-shaped log S versus E_n curve with a minimum near 10 kJ/mol. Surprisingly, the thermal dissociative sticking coefficient predicted by the PC-MURT for CH_4/Ir(111) is roughly 4 orders of magnitude higher than recent measurements on supported nanoscale Ir catalysts at 1 bar pressure, which suggests that substantial improvements in catalyst turnover rates may be possible.

Acknowledgment. This research was supported by the National Science Foundation (NSF) and by the donors of the American Chemical Society Petroleum Research Fund. H.L.A. gratefully acknowledges fellowship support under NSF IGERT grant no. 9972790. We thank Buddie Mullins for helpful discussions and detailed information about the nozzle temperatures and seeding conditions of his beam experiments.

Supporting Information Available: Tables of the experimental data points and the parameters necessary to reproduce the MURT theoretical predictions are included. This material is available free of charge via the Internet at http://pubs.acs.org.

References and Notes

(1) Larsen, J. H.; Chorkendorff, I. *Surf. Sci. Rep.* **1999**, *35*, 165.
(2) Wei, J. M.; Iglesia, E. *J. Phys. Chem. B* **2004**, *108*, 4094.
(3) Wei, J. M.; Iglesia, E. *J. Catal.* **2004**, *225*, 116.
(4) Wei, J. M.; Iglesia, E. *J. Phys. Chem. B* **2004**, *108*, 7253.
(5) Wei, J. M.; Iglesia, E. *J. Catal.* **2004**, *224*, 370.
(6) Wei, J. M.; Iglesia, E. *Phys. Chem. Chem. Phys.* **2004**, *6*, 3754.
(7) Wei, J. M.; Iglesia, E. *Angew. Chem. Int. Ed.* **2004**, *43*, 3685.
(8) Reeves, C. T.; Seets, D. C.; Mullins, C. B. *J. Mol. Catal. A: Chem.* **2001**, *167*, 207.
(9) Seets, D. C.; Reeves, C. T.; Ferguson, B. A.; Wheeler, M. C.; Mullins, C. B. *J. Chem. Phys.* **1997**, *107*, 10229.
(10) Jachimowski, T. A.; Hagedorn, C. J.; Weinberg, W. H. *Surf. Sci.* **1997**, *393*, 126.
(11) Henkelman, G.; Jonsson, H. *Phys. Rev. Lett.* **2001**, *86*, 664.
(12) Au, C. T.; Ng, C. F.; Liao, M. S. *J. Catal.* **1999**, *185*, 12.
(13) Bukoski, A.; Blumling, D.; Harrison, I. *J. Chem. Phys.* **2003**, *118*, 843.
(14) Beck, R. D.; Maroni, P.; Papageorgopoulos, D. C.; Dang, T. T.; Schmid, M. P.; Rizzo, T. R. *Science* **2003**, *302*, 98.
(15) Smith, R. R.; Killelea, D. R.; DelSesto, D. F.; Utz, A. L. *Science* **2004**, *304*, 992.
(16) Bukoski, A.; Harrison, I. *J. Chem. Phys.* **2003**, *118*, 9762.
(17) Abbott, H. L.; Bukoski, A.; Kavulak, D. F.; Harrison, I. *J. Chem. Phys.* **2003**, *119*, 6407.
(18) Abbott, H. L.; Bukoski, A.; Harrison, I. *J. Chem. Phys.* **2004**, *121*, 3792.
(19) Kavulak, D. F.; Abbott, H. L.; Harrison, I. *J. Phys. Chem. B* **2005**, *109*, 685.
(20) Ukraintsev, V. A.; Harrison, I. *J. Chem. Phys.* **1994**, *101*, 1564.
(21) Weinberg, W. H. In *Dynamics of Gas−Surface Interactions*; Rettner, C. T., Ashfold, M. N. R., Eds.; The Royal Society of Chemistry: Cambridge, 1991; Chapter 5.
(22) Sitz, G. O.; Mullins, C. B. *J. Phys. Chem. B* **2002**, *106*, 8349.
(23) Dahl, S.; Logadottir, A.; Egeberg, R. C.; Larsen, J. H.; Chorkendorff, I.; Tornqvist, E.; Norskov, J. K. *Phys. Rev. Lett.* **1999**, *83*, 1814.
(24) Egeberg, R. C.; Ullmann, S.; Alstrup, I.; Mullins, C. B.; Chorkendoff, I. *Surf. Sci.* **2002**, *497*, 183.
(25) Norskov, J. K.; Bligaard, T.; Logadottir, A.; Bahn, S.; Hansen, L. B.; Bollinger, M.; Bengaard, H.; Hammer, B.; Sljivancanin, Z.; Mavrikakis, M.; Xu, Y.; Dahl, S.; Jacobsen, C. J. H. *J. Catal.* **2002**, *209*, 275.
(26) Liu, Z. P.; Hu, P. *J. Am. Chem. Soc.* **2003**, *125*, 1958.
(27) Gee, A. T.; Hayden, B. E.; Mormiche, C.; Kleyn, A. W.; Riedmuller, B. *J. Chem. Phys.* **2003**, *118*, 3334.
(28) Kroes, G. J.; Gross, A.; Baerends, E. J.; Scheffler, M.; McCormack, D. A. *Acc. Chem. Res.* **2002**, *35*, 193.
(29) Gross, A.; Hammer, B.; Scheffler, M.; Brenig, W. *Phys. Rev. Lett.* **1994**, *73*, 3121.
(30) Somers, M. F.; Olsen, R. A.; Busnengo, H. F.; Baerends, E. J.; Kroes, G. J. *J. Chem. Phys.* **2004**, *121*, 11379.
(31) Gross, A.; Wilke, S.; Scheffler, M. *Phys. Rev. Lett.* **1995**, *75*, 2718.
(32) Bukoski, A.; Abbott, H. L.; Harrison, I. Submitted for publication in March, 2005.
(33) Barker, J. R.; Yoder, L. M.; King, K. D. *J. Phys. Chem. A* **2001**, *105*, 796.
(34) Nordholm, S.; Freasier, B. C.; Jolly, D. L. *Chem. Phys.* **1977**, *25*, 433.
(35) Nilsson, D.; Nordholm, S. *J. Chem. Phys.* **2003**, *119*, 11212.
(36) Lenzer, T.; Luther, K.; Reihs, K.; Symonds, A. C. *J. Chem. Phys.* **2000**, *112*, 4090.
(37) Forst, W. *Unimolecular Reactions: A Concise Introduction*; Cambridge University Press: Cambridge, U.K., 2003.
(38) King, D. A.; Wells, M. G. *Surf. Sci.* **1972**, *29*, 454.
(39) Luntz, A. C.; Bethune, D. S. *J. Chem. Phys.* **1989**, *90*, 1274.
(40) Juurlink, L. B. F.; McCabe, P. R.; Smith, R. R.; DiCologero, C. L.; Utz, A. L. *Phys. Rev. Lett.* **1999**, *83*, 868.
(41) Nesbitt, D. J.; Field, R. W. *J. Phys. Chem.* **1996**, *100*, 12735.
(42) Keske, J. C.; Pate, B. H. *Annu. Rev. Phys. Chem.* **2000**, *51*, 323.